Sliding Ferroelectricity in 2D van der Waals Materials: Related Physics and Future Opportunities

Menghao Wu[1*] and Ju Li[2*]

[1]School of Physics, Huazhong University of Science and Technology, Wuhan, Hubei, China 430074

[2]Department of Nuclear Science and Engineering and Department of Materials Science and Engineering, Massachusetts Institute of Technology, Cambridge, MA 02139, USA

Abstract

Near the 100th anniversary of the discovery of ferroelectricity, the so-called "sliding ferroelectricity" has been proposed and confirmed recently in a series of experiments that have stimulated remarkable interest. Such ferroelectricity exists widely and exists only in 2D van der Waals stacked layers, where the vertical electric polarization is switched by in-plane interlayer sliding. Reciprocally, interlayer sliding and "ripplocation" domain wall can be driven by external vertical electric field. The unique combination of intralayer stiffness and interlayer slipperiness of 2D van der Waals layers greatly facilitate such switching while still maintaining environmental and mechanical robustness at ambient conditions. In this perspective, we discuss the progress and future opportunities in this behavior. The origin of such ferroelectricity as well as a general rule for judging its existence, are summarized, where the vertical stacking sequence is crucial for its formation. This discovery broadens 2D ferroelectrics from very few material candidates to most of known 2D materials. Their low switching barriers enable high-speed data writing with low energy cost. Related physics like Moiré ferroelectricity, ferroelectric nonlinear anomalous Hall effect and multiferroic coupling are discussed. For 2D valleytronics, non-trivial band topology, superconductivity, their possible couplings with sliding ferroelectricity via certain stacking or Moiré ferroelectricity also deserve interest. We provide critical reviews on the current challenges in this emergent area.

Ferroelectrics with spontaneous switchable electric polarizations are important candidates for realizing nonvolatile random-access memory. Their bi-stable states with moderate switching barriers may enable memories with room-temperature robustness at nanoscale. A successful combination of ferroelectricity and semiconductor will be highly desirable in the coming era of ferroelectronics[1], which enables ferroelectric field-effect transistor, merging logic and memory functionalities in a single device, overcoming the interconnect bottleneck in von Neumann architecture.

The field of ferroelectricity continues to grow a century after its discovery by Valasek, with emerging new topics. Studies on two-dimensional (2D) van der Waals ferroelectrics since 2013[2,3] offer a possible solution to the well-known epitaxial compatibility problem with the substrate: if the media of ferroelectricity are 2D materials with atomic thickness, also with clean van der Waals interface that does not require lattice match with substrates, they should be exempt from the interfacial issues for device integration. Additionally, many of them are high-mobility semiconductors (>1000 $cm^2 \cdot V^{-1} \cdot s^{-1}$) like phosphorene[4], MoS_2,[5] and InSe[6]. Nevertheless, successful trials in searching for 2D van der Waals ferroelectrics were once limited to very few cases: the electric polarizations of lV-VI monolayers are strictly in-plane,[7-11] and the more favorable vertical ferroelectricity was experimentally confirmed in only $CuInP_2S_6$[12,13] and In_2Se_3.[14-16] After all, the vertical ion displacements for ferroelectric switching is limited in a confined 2D layer.

However, the theory of sliding ferroelectricity proposed in 2017[17,18] reveals the universal existence of vertical ferroelectricity in 2D layers, which has been confirmed in a series of van der Waals systems within several years. Strikingly, herein the vertical ferroelectric switching is induced by in-plane interlayer sliding without any requisite vertical ion displacements, which was unreported in previous ferroelectrics. Such a unique mechanism gives rise to ultra-low switching barriers (~meV/f.u.) that enable high-speed data writing with low energy cost, while the robustness against thermal fluctuations is still ensured. In this perspective, we discuss the research trajectory of sliding ferroelectricity, clarify its origin, and examine its potential and challenges. We suggest promising directions for future research and the broader emerging topics like Moiré ferroelectricity, metallic ferroelectricity, etc.

Theoretical Model

According to the model of sliding ferroelectricity[17,18], for the van der Waals bilayer of many 2D materials, the two layers are actually not identical. Taking the AB stacking boron nitride (BN) bilayer displayed in Fig. 1a as an example, the N atom in the upper layer is over the hexagon center in the down layer, while the B atom in the upper layer is right over the N atom in the down layer (staggered with B over N marked by the black arrow). Such inequality between two layers leads to a *net* interlayer charge transfer and a vertical polarization of 2.08 pC/m by first-principles calculations (0.68 $\mu C \cdot cm^{-2}$ in 3D), which can be switched via interlayer translation by one B-N bond length along either one of the three directions marked by the red arrows (three equivalent reversed states), moving the N atoms in the upper layer right over the B atoms of the down layer, as shown in Fig. 1a.
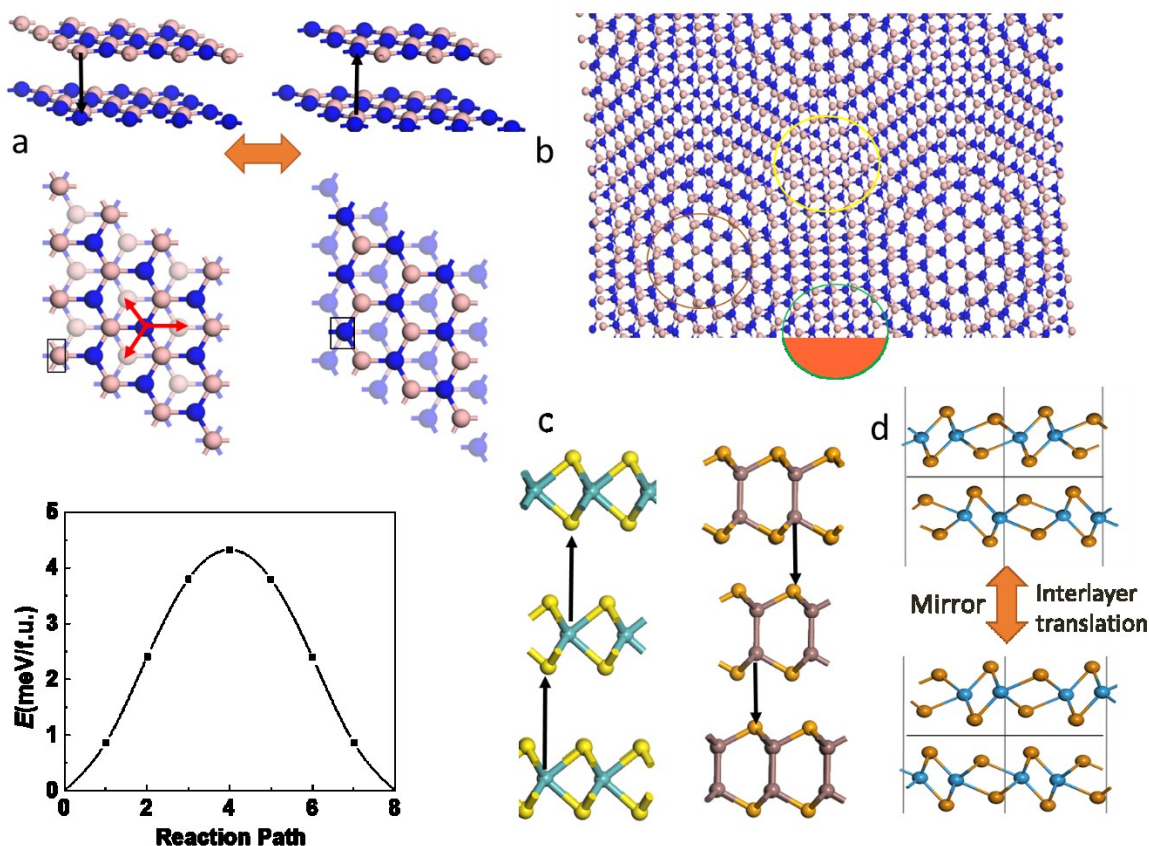
Fig. 1: Mechanism of sliding ferroelectricity. a. Ferroelectric switching pathway of BN bilayer via interlayer sliding. b. Ferroelectric Moiré superlattice in twisted BN bilayer. c. Ferroelectric 3R bulk MoS$_2$ and InSe. (Reproduced with permission.[17] Copyright 2017 American Chemical Society) d. The state obtained via mirror operation with respect to the horizontal plane in the center can also be obtained via interlayer translation for WTe$_2$ bilayer. (Reproduced with permission.[18] Copyright 2018 American Chemical Society)

Table 1. Computed vertical polarizations of AB stacking van der Waals bilayers.[17]

	BN	ZnO	AlN	GaN	SiC	MoS$_2$	InSe	GaSe
Polarization (pC/m)	2.08	8.22	10.29	9.72	6.17	0.97	0.24	0.46

The minimum energy path at the unit-cell level, *i.e.*, the ferroelectric switching pathway, entails an areal energy barrier (*q*) of only around 9meV per unit cell, or few meV/Å^2, which indicates a potentially very small energy cost for data writing. Periodic ferroelectric domains with spatially varying polarization signs can also be formed upon a small-angle twist within the bilayer, as shown in Fig. 1b. In such a Moiré superlattice with large-scale modulation of local stacking, the polarization vanished in AA stacking domains (marked in red circle), while for AB stacking domains, the polarization can be either upwards (in AB-up domains staggered with B over N, marked in yellow circle) or downwards (in AB-down domains

3

staggered with B over N, marked in green circle). Similar types of Moiré patterns for graphene/BN hetero-bilayer can be constructed, where periodic *n* or *p* doped graphene domains can be generated and the electronic properties of graphene can be tuned.

Similar principles can be applied to a series of 2D materials, including most binary compounds with honeycomb lattices, e.g., the already-synthesized graphitic few-layer GaN,[19] SiC[20] and ZnO[21] with much higher computed polarizations, as summarized in Table 1. Van der Waals bilayer like MoS_2, InSe, GaSe, as well as their ground state of 3D bulk phase with R3m symmetry, can also exhibit such sliding ferroelectricity, as shown in Fig. 1c. Meanwhile, they are also semiconductors with suitable bandgaps and high mobility for nanoelectronics, enabling novel in-memory computing device constructs. Aside from honeycomb lattices with three equivalent sliding variants, some other bilayer structures are ferroelectric, but with bi-stable states, e.g., WTe_2 bilayer with a much smaller computed polarization of ~0.38 pC/m.[18] Actually, most van der Waals bilayers or multilayers can be endowed with sliding ferroelectricity with certain stacking-sequence control, and its existence can be judged by using a general principle, as displayed in Fig. 1d: the van der Waals bilayer or multilayer should be non-centrosymmetric, and the equivalent state obtained via mirror operation with respect to the horizontal plane in the center can also be obtained via interlayer translation, revealing a feasible switching pathway of sliding ferroelectricity.

Not all stacking configurations can give rise to ferroelectricity. The aforementioned ferroelectric systems may turn non-polar when the stacking sequence is altered, e.g., to the non-polar AA′ stacking for BN bilayer (eclipsed with B over N) that is almost degenerate in energy compared with polar AB stacking. For bulk phase BN, MoS_2 or InSe stacked by honeycomb monolayers, AA' stacking is non-polar, and the vertical polarization is also missing for AB stacking: the vertical mirror symmetry is preserved in AB stacking bulk phase although the AB layers are not identical, either positively or negatively charged, as revealed by the interlayer differential charge density in Fig. 2a. All the planar layers in the ABC stacking bulk phase are identical and neutral, while their non-symmetric charge density distributions due to the interlayer configuration give rise to vertical polarity. Meanwhile, the AB stacking phase may be transformed to a polar 3R phase (ABC stacking, see 3R MoS_2 in Fig. 1c and 2b) via interlayer translation upon the application of an external electric field. Without limitation by the depolarization field as in 3D ferroelectric material with complex interfaces with the substrate, their bulk polarizations can be greatly enhanced, e.g., the 3R BN possesses a large bulk polarization of 7.6 $\mu C/cm^2$ as listed in Table 2. For 1T/ 1T' transition metal dichalcogenides (TMD) or trihalide monolayers that are centrosymmetric, similarly, their corresponding bulk phase can be either polar or non-polar depending on the stacking phases, e.g., the well-known two phases for SnS_2 and $SnSe_2$ (trigonal and hexagonal phases in Fig. 2c),[22] WTe_2 and ZrI_2 (orthorhombic and monoclinic phases in Fig. 2d)[23], CrI_3 and $CrBr_3$ (R-type and H-type in Fig. 2e)[24]. The non-polar monoclinic WTe_2 can be transformed to polar orthorhombic phase via lateral translation, which cannot be applied to transform the nonpolar trigonal SnS_2 to ferroelectric hexagonal phase, or the nonpolar R-type CrI_3 to ferroelectric H-type. Those phases of different stacking are almost degenerate in energy, so phase control during the synthesis is crucial for the realization of sliding ferroelectricity.
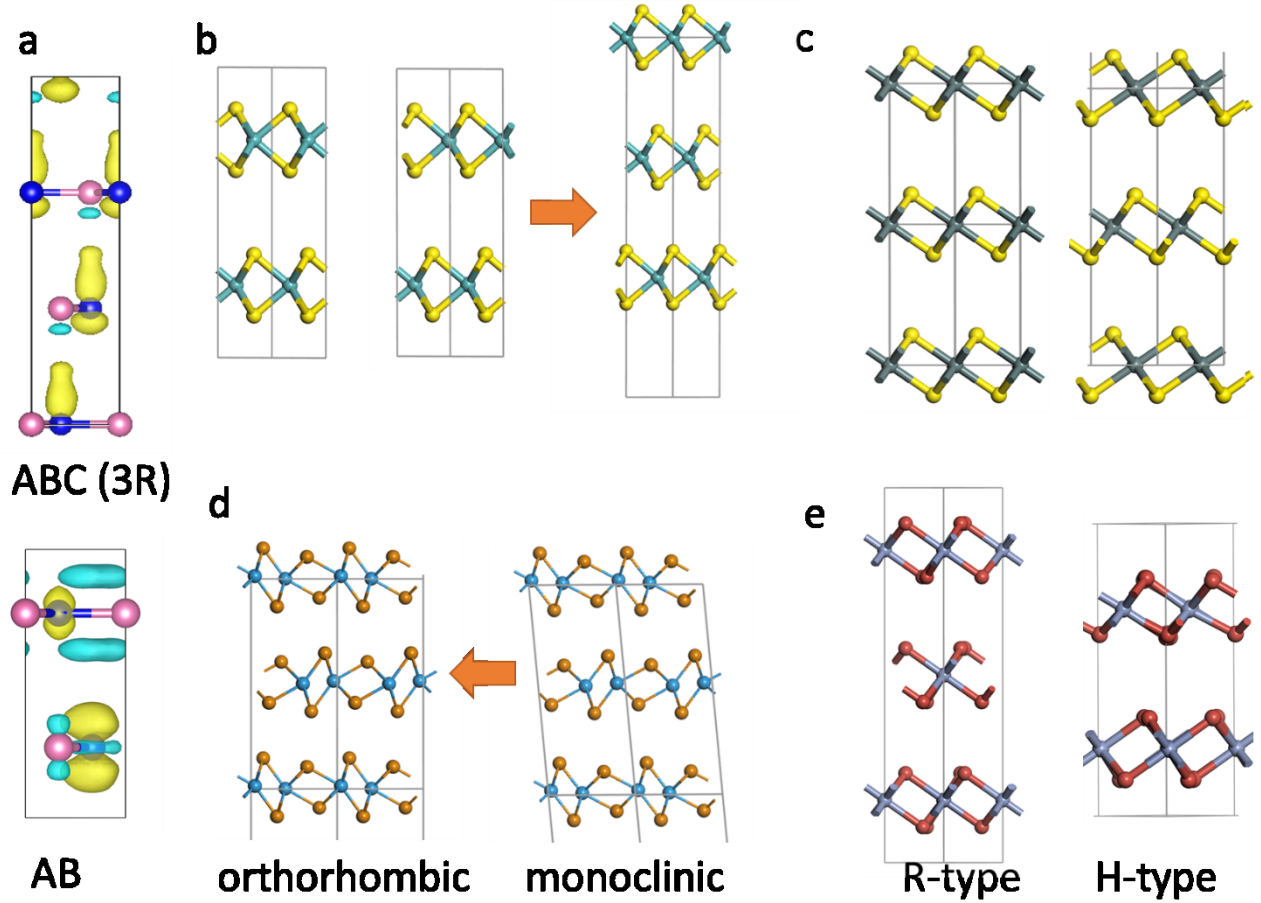
4

Fig. 2: Polar and non-polar phases upon different stacking. a. Interlayer differential charge density of ABC and AB stacking bulk BN, where blue and yellow isosurfaces indicate electron depletion and accumulation after layer stacking, respectively. b. Bulk MoS_2 of different stacking configurations; c. trigonal and hexagonal SnS_2; d. orthorhombic and monoclinic WTe_2; e. R-type and H-type $CrI_3/CrBr_3$.

Table 2. Computed vertical polarizations of van der Waals bulk structures

	3R-BN	3R-MoS$_2$	3R-InSe	h-SnS$_2$	h-SnSe$_2$	h-CrI$_3$	ZrI$_2$
Polarization ($\mu C/cm^2$)	7.6	0.73	0.19	1.13	0.82	0.016	0.31

The kinetics of 2D displacive phase transformations[25] deserve careful discussion. When an externally applied forcing F, e.g. applied vertical electric field or shear stress, is below the athermal threshold[26] F_C for domain switching, the transformation will happen heterogeneously and asynchronously,

assisted by thermal activation. That is to say, there will be a nucleation event and a subsequent growth process of a particular polarization/sliding domain variant, with a finite characteristic nucleation and/or migration activation energy $Q(F<F_C) > 0$, that are related to the domain walls ("ripplocations"[26,27] in the case of 2D sliding ferroelectricity). On the other hand, if the applied field is strong enough, $F \geq F_C$, the transformation will be barrierless and do not need thermal activation[26], $Q(F_C) = 0$, in which case a nucleation-and-growth sequence is not necessary, and the transformation can take place in the entire region almost instantaneously like in spinodal decomposition. Generally speaking, F_C is proportional to q, so a smaller areal energy barrier (in unit of meV/Å^2) means a smaller athermal coercive field. On the other hand, when $F<F_C$ and there is a barrier, the relationship between the absolute activation energy Q (in unit of eV) and q can be somewhat complex and depends on the detailed geometric boundary condition. Here we are talking about one layer sliding over another layer, forming a ripplocation[27] loop as the domain wall, which is both a crystallographic dislocation and potentially a surface ripple in its core region due to out-of-plane buckling. In free-standing bilayer, trilayer, etc. with some excess area "slack" due to pre-compression[28], the formation energy of the ripplocation[27] should be much smaller than standard dislocation or martensitic domain walls in 3D solid, due to the lack of long-range elastic interactions.[25] In fact it has been shown that the standard Frank's law for dislocations: dislocation core energy $\propto |\mathbf{b}|^2$ ($\mathbf{b}$ is the Burgers vector or the sliding displacement in the case of sliding ferroelectricity), no longer works in 2D van der Waals stacked layers, due to the near-complete relaxation of the long-range in-plane elastic energy, by buckling "ripple". The lattice friction (Peierls barrier) to a gliding 2D ripplocation[27] is also expected to be small when q is small. So one can expect facile 2D domain nucleation and growth for certain sub-threshold $F<F_C$. In the case of high-field, $F>F_C$, this issue is largely moot, and the transformation is expected to happen rapidly with appropriate boundary conditions (like Fig. 9c). The non-volatile memory function of sliding ferroelectricity would work well if and only if (a) $Q(F=0) >> 50k_BT$, so when there is zero field, a ferroelectric domain variant state can stay "locked in" despite the thermal fluctuations; and (b) but for certain achievable F (such as < 10 MV/cm vertical electric field), $Q < 5\ k_BT$, so the transformation can be accomplished within nanosecond or even picosecond timescale[28]. Due to the fundamental difference between 2D and 3D dislocations[25], we expect sliding ferroelectricity in 2D van der Waals materials to be both facile under field and non-volatile without field, when appropriate size and geometric boundary condition are implemented to relieve the elastic energy constraints[25], that have long confined 3D martensitic transformations.

Experimental Investigations

The first system where sliding ferroelectricity was experimentally detected was few-layer WTe$_2$ despite its metallicity and relatively small polarization. In 2018, Fei et al. designed a device shown in Fig. 3a, using a graphene monolayer as an electrode that can quantify the polarization of WTe$_2$ bilayer or trilayer below.[29] The graphene conductance is measured when a voltage bias is applied to the bottom gate with the intervening WTe$_2$ grounded. The ferroelectric switching between two vertical polarization states is then revealed by the hysteresis loop in the graphene conductance sensitive to the polarization. The conductance measurements at a series of temperatures indicate its Curie temperature around 350 K, and no bistability is detected in monolayer WTe$_2$. Such device is able to estimate the areal polarization density of WTe$_2$ bilayer (~1×10^4 e/cm=0.16 pC/m measured at 20K), which can be approximately fitted by DFT calculations (~0.38 pC/m) considering the influence of defects, substrate, and thermal fluctuations.[18]
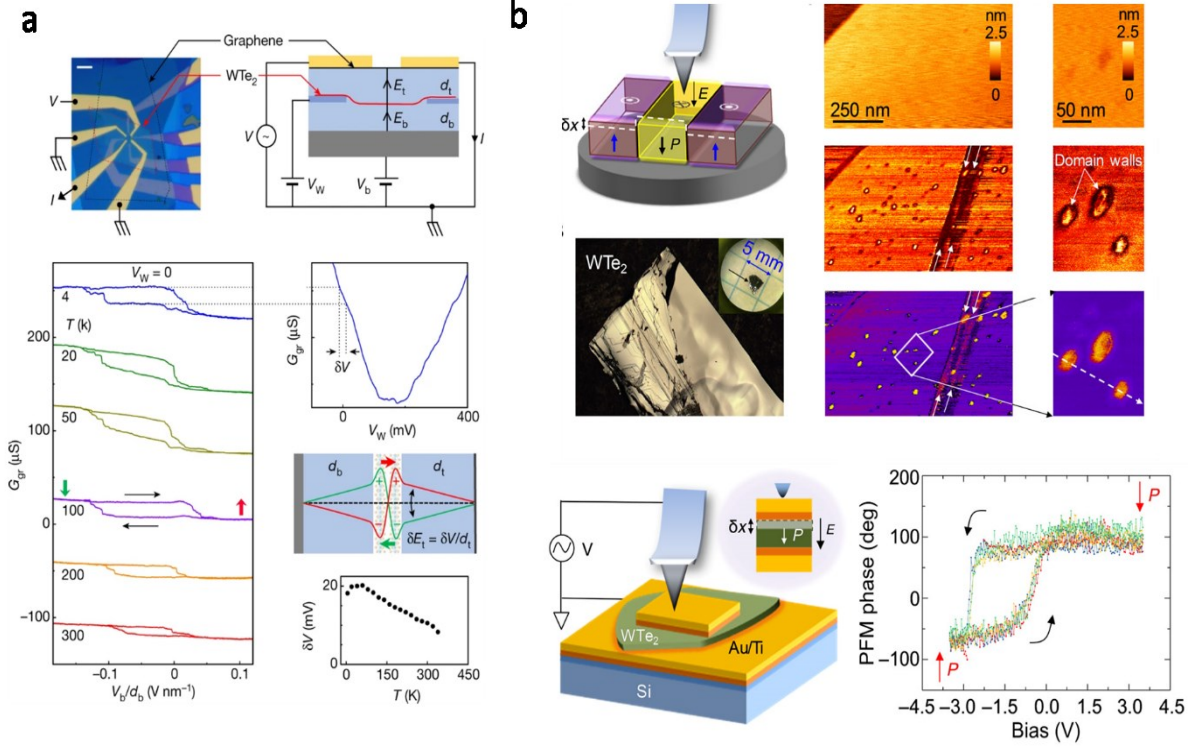
Fig. 3: Detection of ferroelectricity in WTe_2 thin-layer. a. The design of bilayer WTe_2 device with multiply contacted graphene as the top gate, and the measured dependence of graphene conductance on bias exhibiting bistable states associated with the polarization of WTe_2. (Reproduced with permission.[29] Copyright 2018 Nature Publishing Group) b. Device setups and images for probing the ferroelectric domains and bias-dependent piezoresponse phase of WTe_2 flake. (Reproduced with permission.[30] Copyright 2019 AAAS)

In a later report, the vertical ferroelectricity of bulk WTe_2 was further verified by piezoresponse force microscopy (PFM), where the antiparallel ferroelectric domain can be visualized directly as shown in Fig. 3b, implying the existence of bistable polarization states.[30] The domains usually exhibit a distorted circular profile with an average domain size in the range of ~20 to 50 nm, with domain walls that appear as dark lines in the amplitude image. Spectroscopic PFM measurements were performed through the top electrode in a capacitor geometry with WTe_2 multilayer with a thickness around 15nm. The acquired piezoresponse as a function of applied bias shows switchable hysteretic behavior, and the bias-driven, oppositely oriented remnant polarization can be clearly seen in the PFM images of different color contrasts, indicating that the polarization of WTe_2 is switchable under an external bias. The stacking transition during ferroelectric switching in few-layer WTe_2 was confirmed via in situ nonlinear Hall transport measurement utilizing its large Berry curvature near the Fermi level, where the transition via interlayer sliding enables synchronized annihilation and switching of ferroelectric polarization and the Berry curvature.[31]
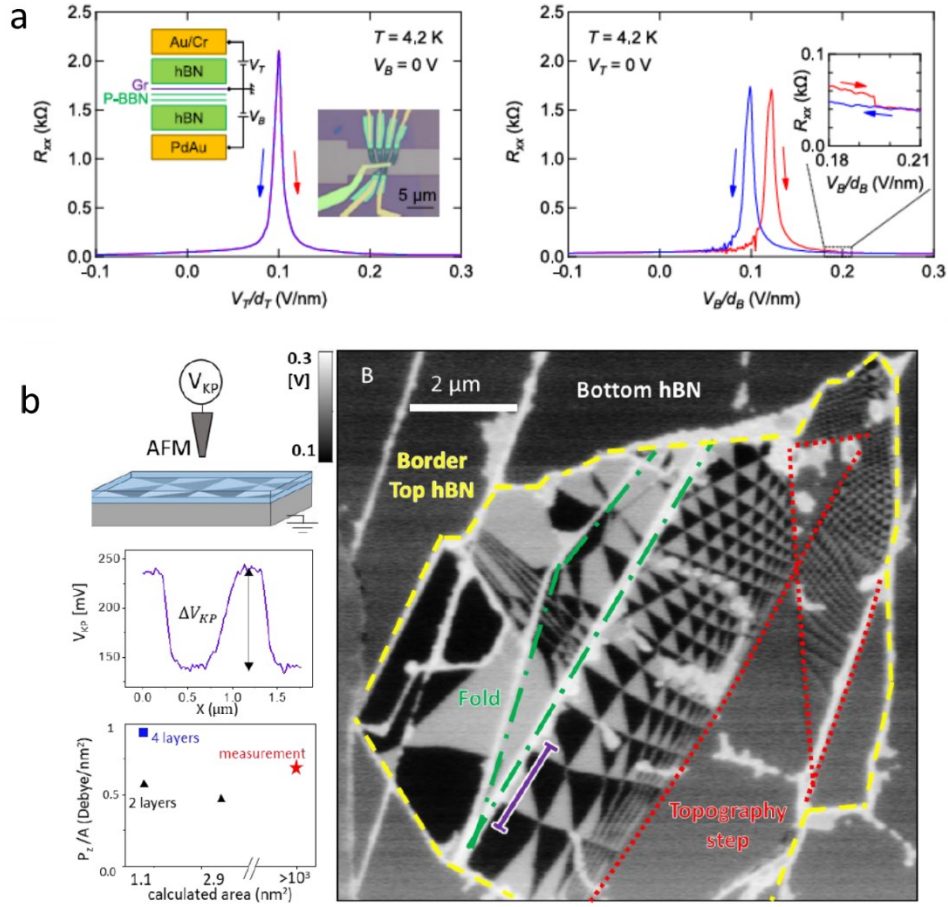
Fig. 4: Detection of ferroelectricity in BN thin-layer. a. The design of dual gated vdW heterostructure device composed of a metal top gate (Au/Cr)/hBN/graphene/0° parallel stacked bilayer BN (P-BBN)/hBN/metal bottom gate (PdAu), and its resistance R_{xx} of graphene as a function of V_T/d_T, with the top gate voltage V_T divided by the thickness of top hBN d_T and the bottom gate voltage VB divided by the distance between graphene and bottom gate electrode d_B. b. Atomic force microscope is operated in Kelvin-probe mode to measure the local potential modulation, at the surface of two 3 nm thick h-BN flakes, which are stacked with a minute twist angle. (Reproduced with permission. [32,33] Copyright 2021 AAAS)

In 2020, the existence of sliding ferroelectricity in BN thin-layers was observed by several research groups. Yasuda et al. designed a dual gated vdW heterostructure device shown in Fig. 4a, using a graphene monolayer as a detector that can quantify the polarization of BN bilayer.[32] The resistance of the graphene sensor as a function of top gate voltage (for both forward and backward gate sweep directions) exhibits a typical maximum without hysteresis. In contrast, the forward and backward scans of the resistance versus the bottom gate voltage show hysteresis, revealing the polarization switching of bilayer BN by the applied electric field. Another case in point is the measured carrier density n_H of graphene extracted from Hall resistance measurements that exhibit hysteretic behavior with an abrupt jump of n_H sweeping V_B, which is almost independent of temperature, up to the room temperature. They also investigated the Moiré pattern of twisted bilayer BN with different stacking domains, which can expand or shrink through domain wall motion upon a vertical electric field.

8

In another report,[33] Stern et al. observed alternating domains of inverted normal polarization around several μm^2 in 3 nm thick BN layers by atomic force microscope (see Fig. 4b) operated in a Kelvin probe mode, which can measure the variations in the electrostatic potential at the surface regions of different stacking configurations. The polarization coupled to lateral sliding can be switched by scanning a biased tip above the surface, where the redistribution of domain-walls to orient the local polarization can be visualized by Kelvin-probe maps. The measured polarizations in both reports on BN layers can fit well with the results predicted by first-principles calculations.

Aside from metallic WTe_2 and insulating BN, the possible existence of sliding ferroelectricity in semiconducting van der Waals layers has also been explored. In a recent report, the amplitude-off and bias-on PFM amplitude and phase hysteresis loops were measured on a 7-nm-thick β-InSe nanoflake at room temperature.[34] A clear amplitude butterfly loop and phase hysteresis loops were observed (see Fig. 5), revealing the switching of vertical polarization. The amplitude hysteresis loop remained as a butterfly-like loop, and the phase switching was still 120° after the sample was exposed to air at room temperature for 1 month. As we learned from the authors of Ref. 32 by private communication, sliding ferroelectricity in some transition-metal dichalcogenides thin-layer are also being investigated.
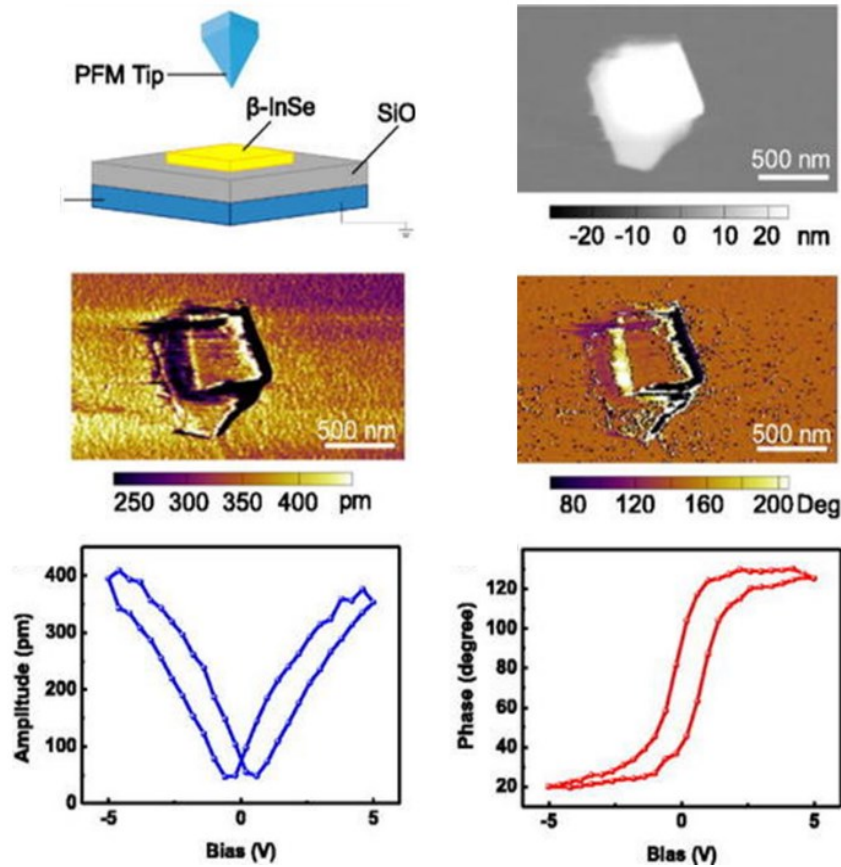

Fig. 5: Detection of ferroelectricity in InSe thin-layer. PFM amplitude and PFM phase hysteresis loops on a 7-nm-thick InSe flake. (Reproduced with permission.[34] Copyright 2019 AIP Publishing)

Related physics

Moiré ferroelectricity

The proposed Moiré ferroelectric domain with spatially varying potential upon a twisted angle in Fig. 1(b) has been observed in both aforementioned reports on ferroelectric BN thin-layers.[32,33] In addition, Woods et al. used electrostatic force microscopy for the visualization of local electric charges on twisted BN bilayer by detecting the variations in the surface potential.[35] Owing to the large potential variation, the regular ferroelectric domains arranged in triangular superlattice can be clearly visualized, as shown in Fig. 6a.
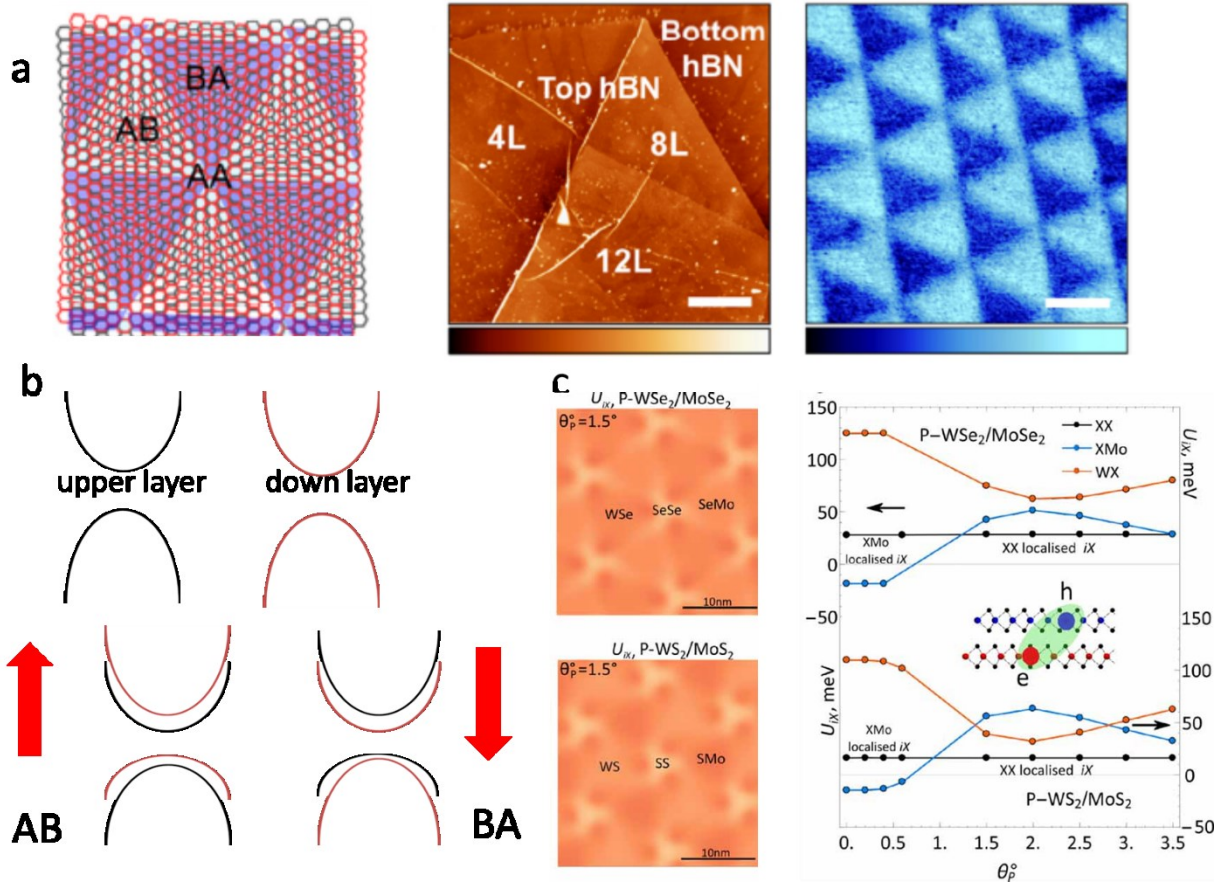

Fig. 6: Moiré ferroelectricity. a. Electrostatic force microscopy image of twisted hBN with triangular potential modulation. (Reproduced with permission.[35] Copyright 2021 Nature Publishing Group) b. Schematic relative shift between the bands of the upper and down layer in different stacking regions of twisted semiconducting bilayer. c. Energy landscapes for interlayer excitons and twist-angle dependence of interlayer exciton energy in different stacking regions of moiré supercell. (Reproduced with permission.[36] Copyright 2021 IOP Publishing Ltd)

Moiré ferroelectricity not only generates periodic *n/p* doped domains and shape the periodicity of the potential energy landscape, but also gives rise to new research focus concerning the coupling between ferroelectricity and twistronic properties, like Moiré flat bands that induce correlation[37] and

superconductivity[38], and the spatially varying bandgaps of twisted bilayer semiconductors driving the exciton flow[39]. For a semiconducting bilayer, a small twist angle creates an internal stacking translation $u(r)$ varying gently with position r that controls the local bandgap $E_g(u(r))$. Aside from the spatially varying interlayer hybridizations, the Moiré potential and local band variation can also be induced by the varying potential of Moiré ferroelectricity, which determines the relative shift between the bands of the upper and down layer in different stacking regions. With the band alignment shown in Fig. 6b. the twisted semiconducting bilayer combined with Moiré ferroelectricity can mimic a quantum dot array with type-II junctions (both in-plane and out-of-plane), which facilitates exciton trapping. A theoretical study[36] revealed the trapping of electrons, holes, and excitons in twisted WX_2/MoX_2 bilayers (X = S, Se), which is attributed to the domain wall networks of Moiré ferroelectricity. Tong et al. predicted bichromatic Moiré potentials for valley electrons, holes, and interlayer trions in $MX_2/M'X'_2/MX_2$ trilayers, with two independently configurable triangular superlattices of neutral excitons with opposite electric dipoles.[40] In a recent experimental study, unconventional ferroelectricity was observed in bilayer graphene sandwiched between two hexagonal BN layers with a Moiré superlattice potential formed at the graphene/BN interface, which is attributed to the electronic correlation effect of Moiré flat bands[41].
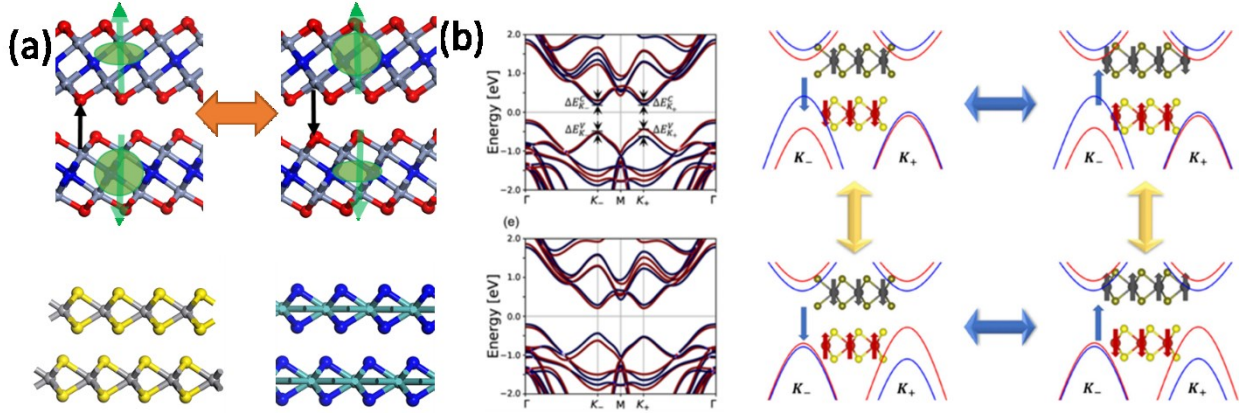

Fig. 7: Sliding multiferroicity. a. Magnetization switching accompanied with ferroelectric switching in Cr_2NO_2, VS_2 and MoN_2. (Reproduced with permission.[17] Copyright 2017 American Chemical Society) b. Valley switching in band structures of VS_2 bilayer associated with ferroelectric and magnetic switching. (Reproduced with permission. [42] Copyright 2020 American Physical Society)

Multiferroicity

Multiferroic materials with robust magnetism and ferroelectricity that are strongly coupled are long-sought but remain elusive to date.[43] For two ferromagnetic monolayers that are anti-ferromagnetically coupled, inequivalent stacking may give rise to both sliding ferroelectricity and uncompensated magnetic moments (see Fig. 7a). The total magnetization can be switched with the reversal of polarization and interlayer voltage, rendering a desirable mode of "electrical writing + magnetic reading". The switchable magnetization for MXene Cr_2NO_2, VS_2 and MoN_2 bilayer are respectively 0.008, 0.016 and 0.09μ_B per unit cell,[17] where μ_B is a Bohr magneton, which is already much larger compared with most type-II mutiferroics.

In a recent study on VS_2 bilayer,[42] the coupling of valley between magnetism and ferroelectricity was noted. As shown in Fig. 7b, owing to the interaction of interlayer ferrovalleys the splitting values at the bottom of the conduction band and the top of the valence band are not equal at valley K_+ and K_-, which will be exchanged via ferroelectric switching or magnetic reversal for both layers. The predicted manipulations of the couplings between electron charge, spin, and valley degrees of freedom are yet to be experimentally validated.

Metallic Ferroelectricity

The multiferroic bilayers mentioned above are mostly metallic (which is the usual case for strong ferromagnets). The coexistence of ferroelectricity and metallicity is forbidden in conventional ferroelectrics as polarization switching upon an external electric field should be hindered by free-carrier screening. This principle also applies to the "ferroelectric metals" proposed by Anderson and Blount[44], referred to as "polar metals" with non-switchable polarization (e.g., $LiOsO_3$[45]). However, the experimentally confirmed sliding ferroelectricity in metallic thin-layer WTe_2 indicates that a thin enough polar metal can be sufficiently penetrated by an electric field for its polarization switching, where the ultra-low sliding barrier may also play an important role. It is likely that most 2D metallic layers can be endowed with a switchable polarization via stacking sequence control (which is yet to be confirmed), and for those properties that do not or scarcely co-exist in pervious insulator ferroelectrics (plasmon, superconductivity, ferromagnetism, etc.), now their possible couplings or interactions with ferroelectricity can be explored.

Ferroelectric Nonlinear Anomalous Hall Effect

For few-layer WTe_2, Wang et al. predicted a remarkable ferroelectric nonlinear anomalous Hall effect where nonlinear anomalous Hall current switches in odd-layer WTe_2 (except for 1T' monolayer) while remaining invariant in even-layer WTe_2 upon ferroelectric transition, which is attributed to the absence and presence of Berry curvature dipole reversal and shift dipole reversal due to distinct ferroelectric transformation in even and odd-layer WTe_2.[46] It was later confirmed[31] by nonlinear Hall effect measurement using the device in Fig. 8, where an applied current flow along the *a*-axis results in the generation of nonlinear Hall voltage along the *b*-axis, proportional to the Berry curvature dipole strength at the Fermi level. Although with similar butterfly-shaped hysteresis in longitudinal conductance, the sign of the nonlinear Hall signal was observed to be reversed in the trilayer while remaining unchanged in the four-layer crystal. Such Berry curvature memory based on sliding ferroelectric systems with non-destructive reading is worthy of further investigation for applications.
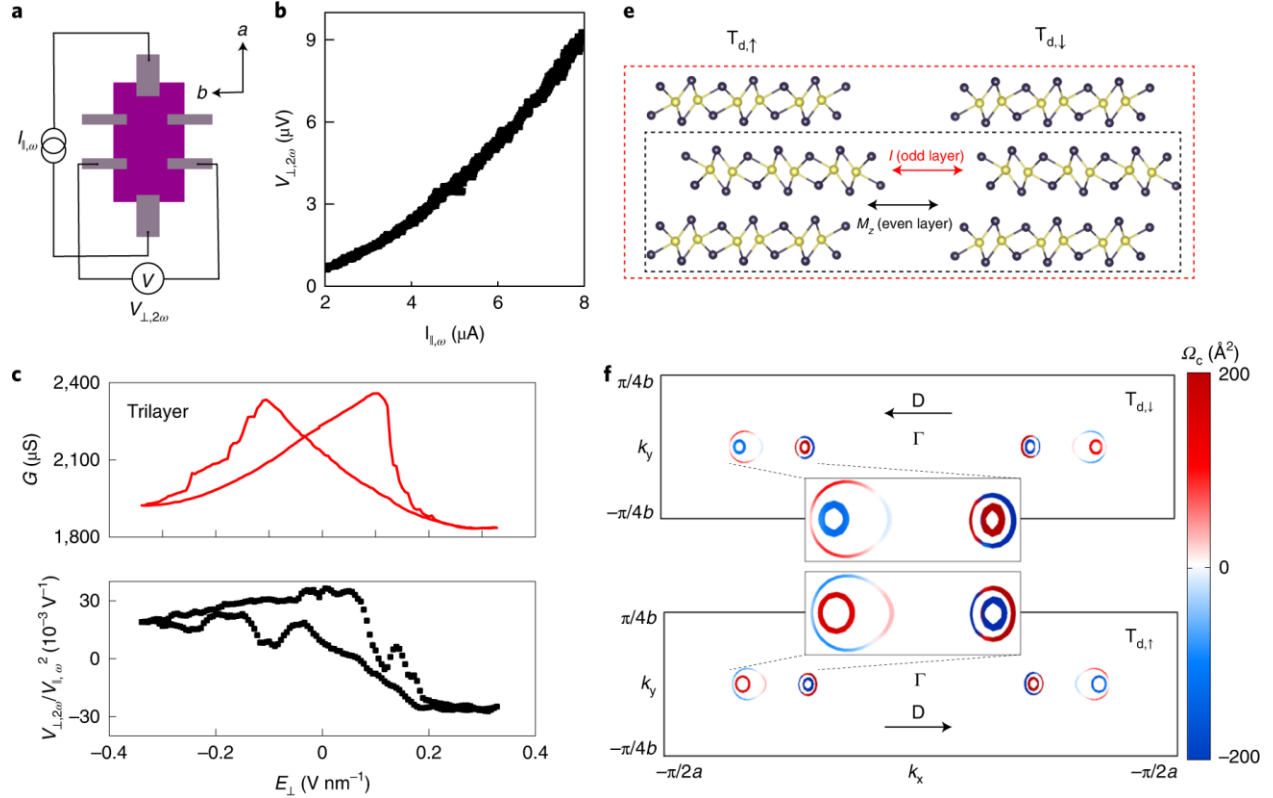
Fig. 8: Ferroelectric nonlinear anomalous Hall effect. Nonlinear Hall effect measurement and calculated Berry curvature distribution at the Fermi level for trilayer and four-layer WTe$_2$. (Reproduced with permission.[31] Copyright 2020 Nature Publishing Group)

Potential Applications

Despite the promise of 2D van der Waals materials in nanoelectronics, it is still unclear which of them will prevail like silicon today. The wide existence of sliding FE ensures that no matter which one, it can be endowed with nonvolatile ferroelectric memory property via certain stacking. The research on sliding ferroelectricity has greatly broadened the candidates of 2D ferroelectrics from very few cases to most 2D materials, ranging from metals to insulators. Boron nitride is widely used as a substrate and gate insulator with high dielectric constant, metallic NbSe$_2$ or WTe$_2$ can be used as 2D electrodes, while InSe and MoS$_2$ can be high-performance semiconductors with suitable bandgaps and high mobility, so they may all possess the function of nonvolatile memory while playing a vital part in devices like field-effect transistors.
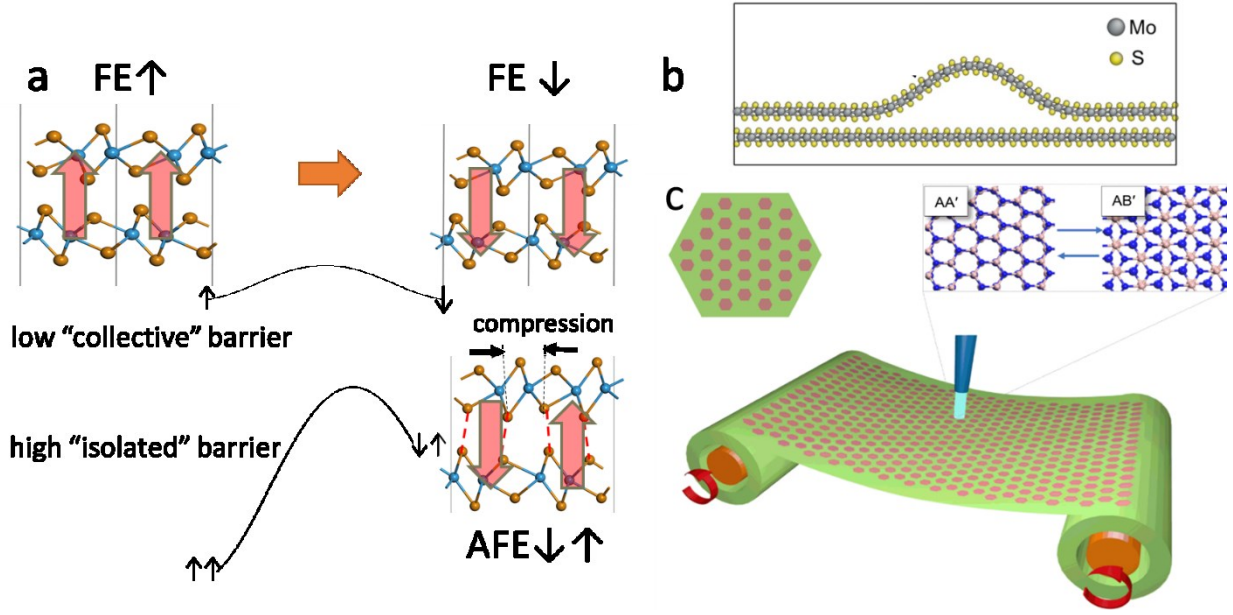
Fig. 9: Low switching barrier with high thermal stability. a. A comparison of ferroelectric switching with a low "collective" barrier, and ferroelectric (FE)-antiferroelectric (AFE) transition with a high "isolated" barrier in WTe$_2$ bilayer. (Reproduced with permission.[18] Copyright 2018 American Chemical Society) b. Ripplocation in MoS$_2$ bilayer. (Reproduced with permission.[27] Copyright 2015 American Chemical Society) c. Optical-driven transition from AA' to AB' stacking in BN bilayer. (Reproduced with permission.[47] Copyright 2020 Springer)

The functional fatigue of current perovskite ferroelectrics has been attributed to their mobile oxygen defects at the interface between ferroelectric oxides and metallic electrodes.[48] For sliding ferroelectric layers, however, the clean van der Waals surface are usually free of such defects, while all the ion displacements are strictly in-plane despite the vertical polarizations are tuned by the perpendicular electrodes. Hence the sliding ferroelectrics should be exempt from this kind of fatigue mechanism.

There is usually a tradeoff in optimizing the performance for data storage when considering the intensive switching barrier q (in unit of meV/Å^3 or meV/Å^2) between ferroic variants: a low q is favorable to reduce the energy cost and enhance the speed for data writing, while also reducing the robustness against thermal fluctuations. For example, the low switching barrier of magnetic memories gives rise to their high-speed writing and thermal instability at nanoscale (like "superparamagnetism"). However, the key quantity for estimating thermal stability is somewhat different from the switching barrier. For the anisotropic Heisenberg model of a ferromagnet with exchange coupling J (usually < ~ 10meV) and single-ion anisotropy K (usually < ~ meV),

$$H = -J \sum_{<i,j>} S_i S_j - K \sum_j \left(S_{jz} \right)^2$$

For each spin with N nearest neighbors, the thermal stability for non-volatility is determined by the "isolated" barrier (=NJ+K) for one spin to flip while all other spins around are fixed, while the switching

barrier controlling the speed and energy cost is the "collective" barrier (=K) where all spins must "simultaneously" switch to the opposite direction.

Similar model can be applied for ferroelectricity. The "collective" switching barriers of all room-temperature ferroelectrics, to our knowledge, are higher than 27 meV/f.u. ($\sim k_B T$/f.u. at 300K), e.g., 0.43 eV/f.u. for $BiFeO_3$.[49] In comparison, the barriers for interlayer sliding are much lower (4.5 meV/f.u. for BN[17] and 0.15 meV/f.u. for WTe_2 bilayer[18]). This has to do with the weak van der Waals interaction between adjacent layers. The intralayer rigidity, on the other hand, lead to high "isolated" barrier and high stability against zero-field volatility (see the case of WTe_2 bilayer in Fig. 9a, where the artificial antiferroelectric state formed by in-plane inhomogeneous strain is highly unstable).[18] This is because as the in-plane stretching modulus is much larger than interlayer shearing modulus, sliding ferroelectricity needs to be quite collective and necessarily involves a relatively large "activation area", and collective defects, namely the ripplocation[27] (see Fig. 9b). However, because of the atomic thickness, the total transformed volume and heat dissipation is still small. Such a unique combination enables pico-second timescale high-speed data writing with experimentally acceptable field strength, as predicted[28,47] and recently shown with opto-mechanical light pulses[50]. Aside from ferroelectric switching between bistable states from AB to BA, the optical-driven transformation between inequivalent stacking orders from AA' to AB' has also been predicted[47] (see Fig. 9c, where the data can be written by laser beam and read by nonlinear Edelstein effect), where the low switching barrier and high robustness are similarly ensured.
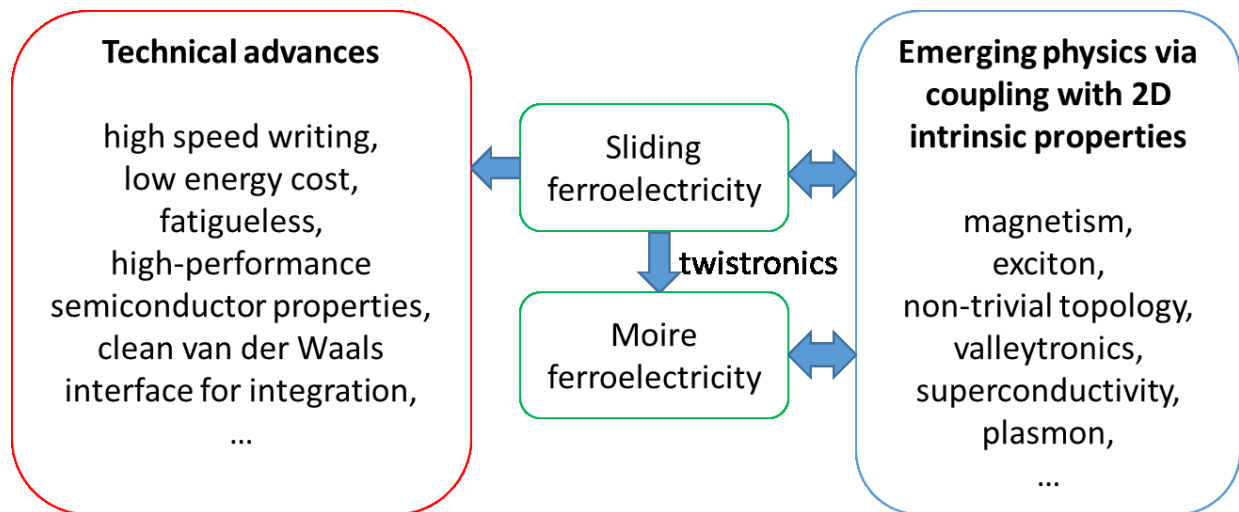

Fig. 10: Schematic diagram of the opportunities in sliding ferroelectricity.

Lastly, we want to comment that interlayer sliding generates large *xz* or *yz* plastic strains, so in the "*xz/yz*" sense, sliding ferroelectricity can also be called sliding *ferroelasticity*. However, *z* is not a Bravais replication direction in 2D van der Waals materials, as only *x* and *y* are extensible. So such a sliding displacement is often considered to be internal shuffling in a 2D Bravais lattice framework. Nonetheless, there will also be in-plane relaxation strains in *xx*, *yy*, *zz* and sometimes even *xy*, slaved to such "internal shuffling"[51] sliding displacement. The coupling between the electric polarization vector, *xz/yz* plastic strain, *xx/yy/xy/zz* relaxation (elastic) strain tensor, and the bending curvature inside ripplocation (flexoelectric effect[25]) make this problem an extremely rich one.

Outlook

In the booming field of 2D ferroelectricity, sliding ferroelectricity is unique in that it exists widely and exists only in 2D van der Waals stacked layers. Without significant vertical ion displacements (except in the ripplocation domain wall core), the vertical polarization can be switched by in-plane interlayer sliding with an ultra-low barrier, which can be utilized for high-speed data writing with low heat dissipation. In addition to its unique switching mode, other related new physics like Moiré ferroelectricity, metallic ferroelectricity, ferroelectric nonlinear anomalous Hall effect, sliding multiferroic couplings are emerging. Actually, for many intrinsic physical properties of 2D monolayers (magnetism, excitonics, non-trivial topology, valleytronics, superconductivity, etc.), their potential couplings with sliding ferroelectricity via certain stacking or Moiré ferroelectricity upon a twisted angle can be worthy of further explorations, as summarized in Fig. 10.

There are still challenges to overcome at this early stage. The van der Waals charge transfer due to interlayer inequality is usually weak, leading to a low magnitude in polarizations. Even for the polarization obtained in BN bilayer that is an order of magnitude higher compared with WTe_2 bilayer, it is still less than one-half of the computed vertical polarization for thin-layer $CuInP_2S_6$ and In_2Se_3, almost two orders of magnitude lower compared with the bulk polarization of $BiFeO_3$. However, it has been shown that even the WTe_2 bilayer with a weak polarization below 0.2 pC/m can give rise to two distinct conductance states when using graphene as a detector[29]. Moreover, many systems with much higher polarizations are yet to be explored via high throughput screening of material database, noting that the computed polarization of AlN bilayer in Table 1, almost 5 times higher than that of BN bilayer, is also the highest vertical polarization of current 2D ferroelectrics known to date.

While a free-standing, slightly slacked geometry in vacuum is theoretically the cleanest to discuss sliding ferroelectricity, in practical applications it might be advantageous to put the 2D van der Waals materials on top of some solid substrate on the bottom, and exposed to some gas environment or solid electrode on the top. The issue of mobile ionic impurities and electronic charge puddles that might segregate on top/bottom interfaces and depolarize the vertical electric dipole is something one has to contend with. Covering relatively inert 2D encapsulations like BN on top and bottom to maintain clean interfaces could be a solution, but this will alter the bending modulus and thus the ripplocation domain wall width, and thus the domain kinetics, from the idealized situation.

To conclude, although large-scale applications in nanoelectronics require simultaneous optimization of high ferroelectric polarizations with low switching barriers, moderate bandgaps with high mobility, low materials/manufacturing cost, non-toxicity, etc., since most 2D materials can be endowed with sliding ferroelectricity via stacking design, there are plenty of candidates for such optimizations on different material platforms. The opportunities are vast for both emerging physics and potential applications.

Author Information

Affiliations

School of Physics, Huazhong University of Science and Technology, Wuhan, Hubei, China 430074

Menghao Wu

Department of Nuclear Science and Engineering and Department of Materials Science and Engineering, Massachusetts Institute of Technology, Cambridge, MA 02139, USA

Ju Li

Corresponding authors

Correspondence to Menghao Wu (wmh1987@hust.edu.cn) or Ju Li (liju@mit.edu)

Ethics declarations

Competing interests

The authors declare no competing interests.

Reference

1   Khan, A. I., Keshavarzi, A. & Datta, S. The future of ferroelectric field-effect transistor technology. *Nature Electronics* **3**, 588-597, doi:10.1038/s41928-020-00492-7 (2020).
2   Wu, M., Burton, J. D., Tsymbal, E. Y., Zeng, X. C. & Jena, P. Hydroxyl-decorated graphene systems as candidates for organic metal-free ferroelectrics, multiferroics, and high-performance proton battery cathode materials. *Phys.Rev.B* **87**, 081406 (2013).
3   Wu, M. & Jena, P. The rise of two-dimensional van der Waals ferroelectrics. *Wiley Interdisciplinary Reviews: Computational Molecular Science* **8**, e1365, doi:10.1002/wcms.1365 (2018).
4   Li, L. *et al.* Black phosphorus field-effect transistors. *Nat. Nano.* **9**, 372-377, doi:10.1038/nnano.2014.35

http://www.nature.com/nnano/journal/v9/n5/abs/nnano.2014.35.html#supplementary-information
(2014).
5   RadisavljevicB, RadenovicA, BrivioJ, GiacomettiV & KisA. Single-layer MoS2 transistors. *Nat. Nano.* **6**, 147-150, doi:http://www.nature.com/nnano/journal/v6/n3/abs/nnano.2010.279.html#supplementary-information (2011).

6   Bandurin, D. A. *et al.* High electron mobility, quantum Hall effect and anomalous optical response in atomically thin InSe. *Nat. Nano.* **12**, 223-227, doi:10.1038/nnano.2016.242

http://www.nature.com/nnano/journal/v12/n3/abs/nnano.2016.242.html#supplementary-information (2017).

7   Wu, M. & Zeng, X. C. Intrinsic Ferroelasticity and/or Multiferroicity in Two-Dimensional Phosphorene and Phosphorene Analogues. *Nano Lett.* **16**, 3236-3241, doi:10.1021/acs.nanolett.6b00726 (2016).

8   Chang, K. *et al.* Discovery of robust in-plane ferroelectricity in atomic-thick SnTe. *Science* **353**, 274 (2016).

9   Chang, K. *et al.* Microscopic Manipulation of Ferroelectric Domains in SnSe Monolayers at Room Temperature. *Nano Lett* **20**, 6590-6597, doi:10.1021/acs.nanolett.0c02357 (2020).

10   Higashitarumizu, N. *et al.* Purely in-plane ferroelectricity in monolayer SnS at room temperature. *Nature Communications* **11**, 2428, doi:10.1038/s41467-020-16291-9 (2020).

11   Bao, Y. *et al.* Gate-Tunable In-Plane Ferroelectricity in Few-Layer SnS. *Nano Lett* **19**, 5109-5117, doi:10.1021/acs.nanolett.9b01419 (2019).

12   Liu, F. *et al.* Room-temperature ferroelectricity in CuInP2S6 ultrathin flakes. *Nat. Commun.* **7**, 12357, doi:10.1038/ncomms12357 (2016).

13   Belianinov, A. *et al.* CuInP2S6 Room Temperature Layered Ferroelectric. *Nano Lett.* **15**, 3808-3814, doi:10.1021/acs.nanolett.5b00491 (2015).

14   Zheng, C. *et al.* Room temperature in-plane ferroelectricity in van der Waals In$_2$Se$_3$. *Science Advances* **4**, doi:10.1126/sciadv.aar7720 (2018).

15   Zhou, Y. *et al.* Out-of-Plane Piezoelectricity and Ferroelectricity in Layered alpha-In2Se3 Nanoflakes. *Nano Lett* **17**, 5508-5513, doi:10.1021/acs.nanolett.7b02198 (2017).

16   Ding, W. *et al.* Prediction of intrinsic two-dimensional ferroelectrics in In2Se3 and other III2-VI3 van der Waals materials. *Nature Communications* **8**, 14956, doi:10.1038/ncomms14956

https://www.nature.com/articles/ncomms14956#supplementary-information (2017).

17   Li, L. & Wu, M. Binary Compound Bilayer and Multilayer with Vertical Polarizations: Two-Dimensional Ferroelectrics, Multiferroics, and Nanogenerators. *ACS nano* **11**, 6382-6388, doi:10.1021/acsnano.7b02756 (2017).

18   Yang, Q., Wu, M. & Li, J. Origin of Two-Dimensional Vertical Ferroelectricity in WTe2 Bilayer and Multilayer. *J. Phys. Chem. Lett.* **9**, 7160-7164, doi:10.1021/acs.jpclett.8b03654 (2018).

19   Al Balushi, Z. Y. *et al.* Two-dimensional gallium nitride realized via graphene encapsulation. *Nat. Mater.* **15**, 1166-1171, doi:10.1038/nmat4742

http://www.nature.com/nmat/journal/v15/n11/abs/nmat4742.html#supplementary-information (2016).

20   Lin, S. Light-emitting two-dimensional ultrathin silicon carbide. *The Journal of Physical Chemistry C* **116**, 3951-3955 (2012).

21   Tusche, C., Meyerheim, H. & Kirschner, J. Observation of depolarized ZnO (0001) monolayers: formation of unreconstructed planar sheets. *Physical review letters* **99**, 026102 (2007).

22   Ma, Z. *et al.* All roads lead to Rome: Sodiation of different-stacked SnS2. *Nano Energy* **67**, 104276, doi:https://doi.org/10.1016/j.nanoen.2019.104276 (2020).

23   Zhou, Y. *et al.* Pressure-induced Td to 1T′ structural phase transition in WTe2. *AIP Advances* **6**, 075008, doi:10.1063/1.4959026 (2016).

24   Chen, W. *et al.* Direct observation of van der Waals stacking–dependent interlayer magnetism. *Science* **366**, 983, doi:10.1126/science.aav1937 (2019).

25   Li, W., Qian, X. F. & Li, J. Phase Transitions in 2D Materials. *Nature Reviews Materials* **in press** (2021).

26   Li, J. The Mechanics and Physics of Defect Nucleation. *MRS Bulletin* **32**, 151-159, doi:10.1557/mrs2007.48 (2007).

27   Kushima, A., Qian, X., Zhao, P., Zhang, S. & Li, J. Ripplocations in van der Waals Layers. *Nano Lett.* **15**, 1302-1308, doi:10.1021/nl5045082 (2015).

28   Zhou, J., Xu, H., Li, Y., Jaramillo, R. & Li, J. Opto-Mechanics Driven Fast Martensitic Transition in Two-Dimensional Materials. *Nano Letters* **18**, 7794-7800, doi:10.1021/acs.nanolett.8b03559 (2018).

29   Fei, Z. *et al.* Ferroelectric switching of a two-dimensional metal. *Nature* **560**, 336-339, doi:10.1038/s41586-018-0336-3 (2018).

30   Sharma, P. *et al.* A room-temperature ferroelectric semimetal. *Science Advances* **5**, eaax5080, doi:10.1126/sciadv.aax5080 (2019).

31   Xiao, J. *et al.* Berry curvature memory through electrically driven stacking transitions. *Nature Physics* **16**, 1028-+, doi:10.1038/s41567-020-0947-0 (2020).

32   Yasuda, K., Wang, X., Watanabe, K., Taniguchi, T. & Jarillo-Herrero, P. Stacking-engineered ferroelectricity in bilayer boron nitride. *Science* **372**, 1458, doi:10.1126/science.abd3230 (2021).

33   Vizner Stern, M. *et al.* Interfacial ferroelectricity by van der Waals sliding. *Science* **372**, 1462, doi:10.1126/science.abe8177 (2021).

34   Hu, H. *et al.* Room-temperature out-of-plane and in-plane ferroelectricity of two-dimensional β-InSe nanoflakes. *Appl. Phys. Lett.* **114**, 252903, doi:10.1063/1.5097842 (2019).

35   Woods, C. R. *et al.* Charge-polarized interfacial superlattices in marginally twisted hexagonal boron nitride. *Nature Communications* **12**, 347, doi:10.1038/s41467-020-20667-2 (2021).

36   Enaldiev, V. V., Ferreira, F., Magorrian, S. J. & Fal'ko, V. I. Piezoelectric networks and ferroelectric domains in twistronic superlattices in WS2/MoS2 and WSe2/MoSe2 bilayers. *2D Materials* **8**, 025030, doi:10.1088/2053-1583/abdd92 (2021).

37   Cao, Y. *et al.* Correlated insulator behaviour at half-filling in magic-angle graphene superlattices. *Nature* **556**, 80-84, doi:10.1038/nature26154 (2018).

38   Cao, Y. *et al.* Unconventional superconductivity in magic-angle graphene superlattices. *Nature* **556**, 43-50, doi:10.1038/nature26160 (2018).

39   Wu, M., Qian, X. & Li, J. Tunable Exciton Funnel Using Moiré Superlattice in Twisted van der Waals Bilayer. *Nano Lett.* **14**, 5350-5357, doi:10.1021/nl502414t (2014).

40   Tong, Q., Chen, M., Xiao, F., Yu, H. & Yao, W. Interferences of electrostatic moiré potentials and bichromatic superlattices of electrons and excitons in transition metal dichalcogenides. *2D Materials* **8**, 025007, doi:10.1088/2053-1583/abd006 (2020).

41   Zheng, Z. *et al.* Unconventional ferroelectricity in moiré heterostructures. *Nature* **588**, 71-76, doi:10.1038/s41586-020-2970-9 (2020).

42   Liu, X., Pyatakov, A. P. & Ren, W. Magnetoelectric Coupling in Multiferroic Bilayer ${\mathrm{VS}}_{2}$. *Physical Review Letters* **125**, 247601, doi:10.1103/PhysRevLett.125.247601 (2020).

43   Lu, C., Wu, M., Lin, L. & Liu, J.-M. Single-phase multiferroics: new materials, phenomena, and physics. *National Science Review* **6**, 653-668, doi:10.1093/nsr/nwz091 (2019).

44   Anderson, P. W. & Blount, E. I. Symmetry Considerations on Martensitic Transformations: "Ferroelectric" Metals? *Phys. Rev. Lett.* **14**, 217-219, doi:10.1103/PhysRevLett.14.217 (1965).

45   Shi, Y. *et al.* A ferroelectric-like structural transition in a metal. *Nature Materials* **12**, 1024-1027, doi:10.1038/nmat3754 (2013).

46   Wang, H. & Qian, X. Ferroelectric nonlinear anomalous Hall effect in few-layer WTe2. *npj Computational Materials* **5**, 119, doi:10.1038/s41524-019-0257-1 (2019).

47   Xu, H., Zhou, J., Li, Y., Jaramillo, R. & Li, J. Optomechanical control of stacking patterns of h-BN bilayer. *Nano Res.* **12**, 2634-2639, doi:10.1007/s12274-019-2500-y (2019).

48   Tagantsev, A. K., Stolichnov, I., Colla, E. L. & Setter, N. Polarization fatigue in ferroelectric films: Basic experimental findings, phenomenological scenarios, and microscopic features. *J. Appl. Phys* **90**, 1387-1402, doi:10.1063/1.1381542 (2001).

49   Ravindran, P., Vidya, R., Kjekshus, A., Fjellvåg, H. & Eriksson, O. Theoretical investigation of magnetoelectric behavior in $\mathrm{Bi}\mathrm{Fe}{\mathrm{O}}_{3}$. *Physical Review B* **74**, 224412, doi:10.1103/PhysRevB.74.224412 (2006).

50   Park, J., Yeu, I. W., Han, G., Hwang, C. S. & Choi, J.-H. Ferroelectric switching in bilayer 3R MoS2 via interlayer shear mode driven by nonlinear phononics. *Scientific reports* **9**, 14919, doi:10.1038/s41598-019-50293-y (2019).

51   Ishii, A., Li, J. & Ogata, S. Shuffling-controlled versus strain-controlled deformation twinning: The case for HCP Mg twin nucleation. *International Journal of Plasticity* **82**, 32-43, doi:https://doi.org/10.1016/j.ijplas.2016.01.019 (2016).